Fuel 180 (2016) 613–623

Contents lists available at ScienceDirect

Fuel

journal homepage: www.elsevier.com/locate/fuel

Full Length Article

Characterization of particle number and mass size distributions from a small compression ignition engine operating in diesel/methane dual fuel mode

Silvana Di Iorio, Agnese Magno *, Ezio Mancaruso, Bianca Maria Vaglieco

Istituto Motori – CNR, Napoli, Italy

HIGHLIGHTS

- Particle number and mass size distributions were detected at exhaust of CI engine operating in DF mode.
- DF operation reduces the number of particles at all operating conditions.
- The size of particles emitted in DF operation is affected by the different pilot combustion phase.
- In-cylinder indicating data analysis of DF combustion explains different particle number and mass at exhaust.

ARTICLE INFO

Article history:
Received 6 April 2016
Received in revised form 20 April 2016
Accepted 21 April 2016
Available online 27 April 2016

Keywords:
Dual-fuel engine
Methane
Combustion
Particle emissions
Number and mass size distributions

ABSTRACT

The use of gas fuels in compression ignition engines through dual fuel technology represents a promising way to reach a good compromise among sustainable development, energy conservation and environmental preservation. Dual fuel is an operation mode in which the gas, the primary fuel, is mixed with air in the intake manifold before entering into the cylinder. The air–fuel mixture is then ignited by a small amount of liquid fuel directly injected in the cylinder towards the end of the compression stroke. Methane is particularly attractive because of its potential to reduce particulate emissions that are likely the most critical issue of diesel engine exhaust. The present work deals with an experimental activity carried out on a compression ignition engine modified to run in diesel/methane dual fuel mode. The engine is a three-cylinder, 1.0 L of displacement, equipped with a common rail injection system. Experiments were carried out at different engine speeds and loads. For each engine speed, a fixed part of the total energy was supplied by the diesel combustion and the remaining by varying the concentration of methane in the intake. Thermodynamics analysis of the combustion process was performed by in-cylinder pressure signal. Particulate matter emissions were measured at the exhaust by commercial instruments. The sizing and the counting of the particles were performed in the diameter range 5.6–560 nm. It was found out that the effect of diesel/methane combustion on particle formation is strongly affected by the operating condition. In particular, it arose that DF combustion emits lower amount of particles whose size with respect to diesel fuel is related to the different combustion evolution.

Abbreviations: AFR_{st}, stoichiometric air fuel ratio; ATDC, after top dead center; BSFC, brake specific fuel consumption; cad, crank angle degree; CH_4, methane; CI, compression ignition; CO, carbon monoxide; CoV, coefficient of variation; CO_2, carbon dioxide; CN, cetane number; CR, common rail; D, diesel; DEED, Dekati Engine Exhaust Diluter; DF, dual fuel; D_m, mean particle diameter; DOC, diesel oxidation catalyst; DOI, duration of injection; D_p, particle diameter; DPF, diesel particulate filter; ECU, electronic control unit; EEPS, Engine Exhaust Particle Sizer; EGR, exhaust gas recirculation; FSN, filter smoke number; imep, indicated mean effective pressure; λ, relative air–fuel ratio; LHV, lower heating value; $\dot{m}$, mass flow rate; M, total particle mass; MHC, methane hydrocarbons; N, total particle number; NO, nitrogen monoxide; NO_x, nitrogen oxides; PES, percentage energy substitution; P_b, brake power output; PM, particulate matter; PMP, particle measurement programme; PMSDF, particle mass size distribution function; PNSDF, particle number size distribution function; ROHR, rate of heat release; ρ, density; SM, smoke meter; SOC, start of combustion; SOI, start of injection; T_b, brake torque output; TDC, top dead center; THC, total hydrocarbons.

* Corresponding author.
E-mail address: a.magno@im.cnr.it (A. Magno).

http://dx.doi.org/10.1016/j.fuel.2016.04.108
0016-2361/

1. Introduction

Compression ignition (CI) engines play an important role in transportation and power generation because of their high efficiency, affordability, and reliability [1]. Nowadays, most of the research on CI engines is focused on the potential of alternative fuels, both liquid and gaseous, to reduce the dependence from diesel fuel [2,3]. The exigency of a viable alternative to fossil fuels is mainly due to the depletion of petroleum reserves and to environmental problems attributable to exhaust emissions. Besides them, other issues such as increasing fuel price, the need of supplying the fuel demand from local sources reducing the import of crude oil have prompted for the fuel diversification [4].

Methane is particularly attractive as alternative fuel for CI engines because of its renewable nature and clean burning qualities [5]. The most suitable way to utilize it without relevant technological modifications is the dual fuel (DF) concept: because of its poor ignition characteristics, methane cannot totally replace diesel but it can be used as supplement to the liquid fuel. In diesel/methane DF operation, in fact, the gas fuel is injected into the intake manifold to mix uniformly with air; the premixed air–methane mixture is drawn into the cylinder and it is ignited by diesel fuel injected directly in the chamber around the top dead center (TDC) [3].

Diesel piloted combustion of methane allows to reduce the pollutants of most concern for a CI engines that are nitrogen oxides (NO_x) and particulate matter (PM) [6]. Moreover, DF operation benefits of lower carbon dioxide (CO_2) with respect to conventional diesel mode [7]. The main limitations of diesel/methane DF combustion are the high carbon monoxide (CO) and total hydrocarbon (THC) emissions, the latter consisting mainly of methane hydrocarbons (MHC) [8]. The use of after-treatment devices such as diesel oxidation catalyst (DOC) could help to overcome the drawbacks of the high CO. On the other hand, typical DOCs are not very effective with MHC abatement since methane is the most stable of the hydrocarbons. Catalysts covered with much higher precious metal loadings, in fact, could be more efficient for breaking down methane molecules [9]. Some solutions have been suggested to limit both CO and THC emissions making DF fuelling more attractive. Papagiannakis [10] proved through experimental and numerical investigations that air inlet preheating combined to exhaust gas recirculation (EGR) can reduce CO without compromising significantly nitrogen monoxide (NO) emissions. Abedelaal et al. [11] showed that EGR contributes to reduce THC emissions by enriching the air-fuel mixture. Advanced diesel pilot injection was proposed by Yang et al. [12] to reduce the high CO and THC emissions. Biodiesel was used as pilot fuel instead of diesel contributing to a reduction of CO, THC and PM with a small penalty in NO_x emissions [13–15].

Overall, several experimental and theoretical studies have presented performance and emission characteristics of CI engines operating in DF mode at different load settings and engine rotational speed combinations [16–19]. Optical diagnostics have been also applied to have a better understanding of DF combustion behavior and pollutant formation mechanisms [20–22]. However, the most of available literature is concentrated on heavy-duty engines [3] highlighting the necessity of more intensive studies on the application of DF technology to smaller size engines. Moreover, in most of literature there is a lack of data on particle size distributions from DF combustion systems. All research works agree that DF operation leads to a significant reduction of particulate mass concentration with respect to conventional diesel mode but little information is available on the effect of methane addiction to diesel fuel on particle size and number. Nevertheless, particle emissions represent a critical issue in particular for CI engines because of their effect on human health [23]. They were recognized as carcinogen by the World Health Organization [24] and it was demonstrated that particles toxicity increases with decreasing of their size [25]. Moreover, the need to characterize particles emitted from internal combustion engines is driven by the new emission regulations that involve a number based approach in addition to the mass based one [26]. Graves et al. [27] found out that soot aggregates from DF combustion have similar primary particle size, aggregate size, and effective density as diesel soot thus suggesting diesel particulate filter (DPF) as an effective mean to reduce these emissions. The main drawback of the DPF regards the management of the regeneration process. As the particles are trapped, the filer becomes clogged and the exhaust backpressure increases leading to the decrease of the engine efficiency. The loaded soot is eliminated by means of the regeneration during which particle emissions increase as well as fuel consumption [28]. Hence, it is important to reduce the PM emissions just at engine out and to reduce the regeneration frequency. This goal could be achieved by diesel/methane DF technology.

The aim of the paper is the characterization of a diesel/methane dual fuel operation in terms of performance and particle emissions. The novelty of the present research activity consists mainly on the analysis of the effect of diesel/methane DF combustion on particle size and number. The investigation was carried out on a small size CI engine properly modified to run in DF mode: a gas injector was installed in the intake manifold and it was managed by a delay unit developed in Istituto Motori while the original electronic control unit (ECU) for diesel injection control was retained. Experiments were performed at the engine speeds of 1600, 2800 and 3200 rpm and at 30%, 50% and 70% of the rated torque output. The engine was first operated in conventional mode with neat diesel fuel and then in diesel/methane DF configuration. Under DF mode, at a fixed engine speed sufficient amount of diesel fuel was injected to cover the 10% of the maximum torque output. The remaining percentage of the desired torque output was achieved by changing the amount of methane. Combustion behavior of DF combustion was analyzed through indicating data. A smoke meter was used to evaluate PM concentration. The sizing and the counting of the particles were performed in the range from 5.6 to 560 nm.

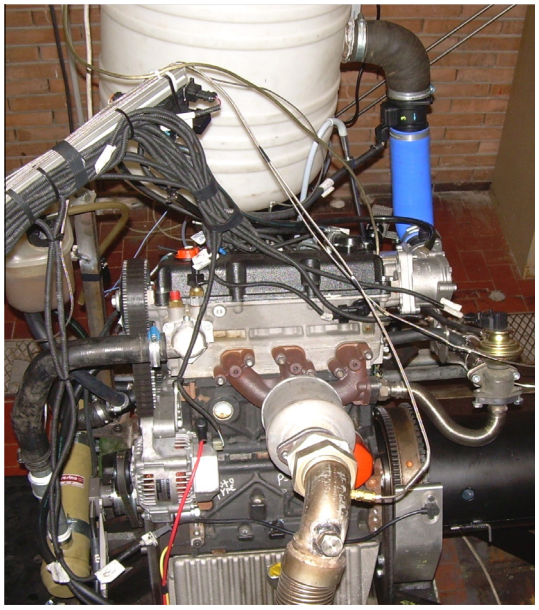

Fig. 1. Test engine.

Table 1
Engine specifications.

Engine	Compression ignition
Number of cylinders	3, in-line
Bore (mm)	75.0
Stroke (mm)	77.6
Displacement (cm^3)	1028
Compression ratio	17.5:1
Max. power (kW)	15 @ 3600 rpm
Max. torque (Nm)	60 @ 2000 rpm
Injection system	Direct, common rail
Max. injection pressure (bar)	1400
Aspiration	Naturally aspirated
Intake valves opening (cad BTDC)	13
Intake valves closing (cad ATDC)	39
Exhaust valves opening (cad BTDC)	38
Exhaust valves closing (cad ATDC)	14

2. Experimental apparatus and procedures

2.1. Test engine

The investigation was carried out on a three-cylinder, six valves, 1.0 L, CI engine for quadricycle vehicle (Fig. 1). Details about engine specifications are listed in Table 1. The engine was equipped with an electronically controlled common rail (CR) injection system characterized by a unit pump operated by a three-lobe cam that allows to reach a maximum injection pressure of 1400 bar. The engine was naturally aspirated; the intake air was drawn from a tank in order to reduce the pressure oscillations. In the original configuration, the engine was provided with two emission reduction systems: cooled EGR for NO_x reduction and a diesel DOC for CO and THC abatement.

In order to carry out diesel/methane DF experiments, the intake manifold was modified to set up a 4 holes injector suitable for gaseous fuels characterized by dynamic flow rate of 2000 cm^3/min at 4 bar. Methane was charged in a compressed bottle at 200 bar and decompressed to 4 bar through a regulator and, then, supplied to the intake manifold. The injector was managed by a control unit, developed in Istituto Motori that allowed the setting of the number of injections, the start (SOI) and the duration of injection (DOI) synchronized with each engine combustion cycle. Methane was injected in the intake manifold at 10 crank angle degrees (cad) after top dead center (ATDC) of each cylinder. For diesel fuel, a commercial injector was used; the injection strategy, i.e. SOI, DOI and injection pressure, varied according to the engine operating condition.

2.2. Test facilities

The engine torque was measured with a resolution of 1 Nm by a dynamometer load cell (STIPAF L3B160 M) characterized by maximum power of 93.2 kW and a maximum engine speed of 5300 rpm. The temperatures of engine coolant, air inlet and exhaust were measured by type K thermocouples (OGDEN series 121HT MGO) with a resolution of 1 K. Diesel fuel consumption was measured by a gravimetric balance (AVL730) at a frequency of 10 Hz and with an accuracy of 0.12%. Methane fuel consumption was measured by thermal mass flow meters (Brooks SLA 5861) with an accuracy of 1%. In order to monitor the combustion evolution, in-cylinder pressure signals were detected by quartz transducers (AVL GH14P) characterized by sensitivity of 15.6 pC/bar and natural frequency of 130 kHz. They were flush-mounted in the head in all the cylinders by means of glow plug adaptors. The pressure signals of 500 cycles were recorded with a resolution of 0.2 cad by a high-speed data acquisition system (AVL Indimodul) synchronized with the crankshaft position through the signals transmitted by an optical shaft encoder (AVL365C).

An AVL smoke meter 415S was used to measure the FSN that was converted in PM concentration (mg/m^3) through empirical relations. The smoke meter was characterized by a resolution of 0.001 FSN/0.01 mg/m^3 and a measuring range of 0–10 FSN corresponding to 0–32,000 mg/m^3.

Particle number and electrical mobility diameters were measured by means of the Engine Exhaust Particle Sizer 3090 (EEPS) developed by TSI (Table 2). The instrument draws a sample of the exhaust flow into the inlet continuously. Particles are positively charged to a predictable level using a corona charger. Charged particles are then introduced to the measurement region where at the center there is a high-voltage electrode column. A positive voltage is applied to the electrode creating an electric field that repels the positively charged particles outward according to their electrical mobility. Charged particles strike the respective electrometers and transfer their charge. Particles with higher electrical mobility strike the electrometers at the top, whereas, particles with lower electrical mobility strike the electrometers lower in the stack.

The charging and mobility classification characteristics of the EEPS define the instrument matrix that is used to invert the measured electrometer currents to particle size distributions. Measurements were performed by using a proper matrix taking into account that the engine exhaust particles, specifically carbonaceous agglomerates, differ from spherical particles because agglomerates uptake more charge than spheres at a given mobility diameter [29].

Before entering the EEPS, the sample of exhaust gas was taken by a 1.5 m long line heated at 150 °C and it was diluted by the Dekati Engine Exhaust Diluter (DEED), a Particle Measurement Program (PMP)-compliant conditioning system. In the dilution system, the sample is first diluted with air heated above 150 °C. Then, the sample passes through an evaporation chamber at a temperature above 300 °C for removing volatile particles. After the thermal conditioning, the sample is further diluted to reduce the particle concentration along with the temperature to a suitable level for the aerosol particle sensors for size distribution measurement.

2.3. Test fuels

The engine was fuelled with commercial diesel fuel in conventional operation mode and, simultaneously, with diesel and methane in DF mode. Methane was stored in a pressurized bottle with a purity level of 99.95%; the impurities contained in the methane are reported in Table 3.

Table 4 shows the main physicochemical properties of the tested fuels. Methane has 17% higher lower heating value (LHV) and 18% higher stoichiometric air fuel ratio (AFR_{st}) than diesel fuel resulting in lower heating value of stoichiometric mixture for methane with respect to diesel fuel. Methane has different ignition

Table 2
Particles measurement system specifications.

Instrumentation	TSI EEPS
Particle size range	5.6–560 nm
Particle size resolution	16 channels per decade (32 total)
Time resolution	10 size distributions per second
Electrometer channels	22

Table 3
Impurities in methane bottle.

Species	CO_2	CO	N_2	O_2	H_2O	C_nH_m
(ppm)	<5	<2	<20	<2	<5	<15

Table 4
Test fuels physico-chemical properties.

Properties	Diesel	Methane
Chemical formula	$C_nH_{1.8n}$	CH_4
Density @ 15 °C (kg/m^3)	834.5	0.678
Viscosity @ 40 °C (mm^2/s)	3.34	–
Lower heating value (MJ/kg)	42.8	50.0
AFR_{st}	14.2	17.2
Auto-ignition temperature (°C)	220	650
Flammability limits (% vol)	0.6–7.5	5–15
Cetane number	55.1	–
Octane number	–	>120
C (% mass)	84.71	75
H (% mass)	13.89	25
O (% mass)	1.24	–
N (% mass)	0.16	–

characteristics with respect to diesel fuel due to its lower cetane number (CN) and higher auto-ignition temperature. Moreover, methane contains less carbon per energy input than diesel fuel making it a more environmentally friendly fuel.

2.4. Test method

Before starting the experiments, the engine was warmed up until the coolant temperature reached 80 °C. For all test cases, the inlet air temperature and humidity were about 23 °C and 45%, respectively. EGR was mechanically deactivated and exhaust measurements were performed at raw exhaust in order to isolate the effect of methane on combustion evolution and pollutant formation. Measurements were taken at three engine speeds, 1600, 2800 and 3200 rpm, and at three different loads corresponding to 30%, 50% and 70% of the maximum torque output. Experiments were first performed by running the engine with diesel fuel in order to provide a baseline data set for comparing diesel/methane operations. Under DF mode, 10% of the full load, about 5 Nm, was provided by diesel combustion, the remaining load was supplied by methane. In particular, in order to reach the fixed torque output, the amount of gas fuel was properly changed by controlling the injection duration. Details about the operating conditions are shown in Table 5.

Table 6 reports some characteristic parameters of the tested operating conditions, for both diesel (D) and DF operation, such as the methane percentage energy substitution (PES), the brake specific fuel consumption (BSFC) and the relative air–fuel ratio (λ), calculated as follows:

$$PES = \frac{\dot{m}_{CH_4} \cdot LHV_{CH_4}}{\dot{m}_{CH_4} \cdot LHV_{CH_4} + \dot{m}_{diesel} \cdot LHV_{diesel}} \times 100\% \quad (1)$$

$$\lambda = \frac{\dot{m}_{air}}{AFR^{st}_{CH_4} \cdot \dot{m}_{CH_4} + AFR^{st}_{diesel} \cdot \dot{m}_{diesel}} \quad (2)$$

$$bsfc = \frac{\dot{m}_{CH_4} + \dot{m}_{diesel}}{P_b} \quad (3)$$

The PES index represents the fraction of the total fuel energy that is provided by the methane: at fixed engine speed, it increases with load since the diesel energy input is fixed and more methane is injected to reach the desired torque output.

The λ values reveal a poor air–fuel mixture at all operating conditions and at fixed engine speed, λ decreases when the load increases. Moreover, DF combustion is characterized by lower λ than diesel fuel at the same speed and torque output since lower air mass flow rate was entrained in the cylinder because replaced by methane.

Table 6
Characteristic parameters.

Fuel	Speed (rpm)	$T_b/T_{b,max}$ (%)	T_b (Nm)	PES (%)	λ	BSFC (g/kWh)
D	1600	30	16	–	3.4	312.9
DF		30	16	57.1	2.5	408.4
D		50	26	–	2.6	261.2
DF		50	26	66.7	2.2	274.0
D		70	36	–	1.8	253.9
DF		70	36	69.0	1.6	248.1
D	2800	30	15	–	3.4	354.4
DF		30	15	51.7	2.6	453.7
D		50	25	–	2.8	271.7
DF		50	25	59.8	2.1	308.7
D		70	35	–	2.2	259.4
DF		70	35	64.2	1.8	261.2
D	3200	30	14	–	3.4	380.7
DF		30	14	46.0	2.4	485.7
D		50	24	–	2.7	299.2
DF		50	24	56.2	2.1	334.1
D		70	33	–	2.2	270.6
DF		70	33	60.9	1.7	299.0

Table 5
Operating conditions.

Fuel	Speed (rpm)	T/T_{max} (%)	SOI_{pilot} diesel (cad)	DOI_{pilot} diesel (μs)	SOI_{main} diesel (cad)	DOI_{main} diesel (μs)	p_{inj} diesel (bar)	$\dot{m}_{diesel}$ (kg/h)	$\dot{m}_{CH4}$ (kg/h)
D	1600	30	−10.4	354	2.4	479	464	0.87	–
DF							400	0.50	0.56
D	1600	50	−10.4	354	2.4	479	656	1.15	–
DF							400	0.45	0.76
D	1600	70	−10.4	354	2.4	479	758	1.51	–
DF							400	0.52	1.00
D	2800	30	−22.2	321	−4.4	464	435	1.56	–
DF							400	1.02	0.94
D	2800	50	−22.2	321	−4.4	464	760	2.03	–
DF							400	1.02	1.31
D	2800	70	−22.2	321	−4.4	464	923	2.59	–
DF							400	1.05	1.61
D	3200	30	−33	344	−10.4	510	420	1.85	–
DF							400	1.34	0.98
D	3200	50	−33	344	−10.4	510	793	2.38	–
DF							400	1.28	1.41
D	3200	70	−33	344	−10.4	510	1045	2.90	–
DF							400	1.35	1.81

At low load, DF operation shows about 30% higher BSFC than diesel fuel at all engine speeds investigated; this behavior points out a not efficient gas fuel combustion due to the lower in-cylinder temperature and the lean air fuel mixture that slow down the methane flame propagation. However, the differences in the BSFC values between diesel and DF mode decrease at medium and especially at high load: DF operation has similar (at 2800 rpm–35 Nm) and even lower (at 1600 rpm–36 Nm) BSFC with respect to diesel fuel. The increased combustion temperature and the enrichment of the mixture, in fact, enhance the flame propagation thus resulting in a more efficient combustion.

2.5. Uncertainty analysis

To estimate the reliability of measurements, pressure data of 500 consecutive cycles were recorded for each test point and the averaged pressure cycle was calculated. All other parameters (fuel consumption, temperature, emissions, etc.) were detected for three repetitions. The coefficient of variation (CoV) of each measured quantity was calculated as the ratio of the standard deviation to the mean value; the maximum CoV of each parameter among all the test points [30] are reported in Table 7 revealing a good repeatability.

3. Experimental results

The in-cylinder pressure measurement is an effective tool to analyze the engine behavior since the pressure history directly influences the power output and the engine out emissions. When diesel/methane DF operation is investigated, it is necessary to take into account that methane and diesel fuel have different physico-chemical properties resulting in different combustion development. DF combustion, in fact, includes both diffusive combustion of the high CN liquid fuel and the premixed combustion of the high octane number (ON) gas fuel [15].

In the present research activity, pressure signals were detected in the three cylinders; negligible differences were observed in the pressure traces of the three cylinders in both diesel and diesel/methane fuelling. The rate of heat release (ROHR) and the bulk temperature were calculated by pressure data through the first law of thermodynamics and the perfect gas law [1]. In Fig. 2, indicated data of the second cylinder are plotted for conventional diesel and DF operation at all the investigated conditions. In conventional diesel operation, pressure histories exhibit two peaks due to the combustion of pilot and main fuel. When the engine runs in DF mode two peaks are still distinguishable because two diesel injections occur providing two different ignition sources for the air/methane charge. At all investigated conditions, DF combustion is characterized by slightly lower pressure during the compression stroke. This trend could be due to the higher specific heat capacity ratio of methane with respect to the air resulting in lower charge temperature and, hence, lower in-cylinder pressure. Because of the longer ignition delay, DF combustion process occurs late in the piston down stroke thus showing lower pressure rise and lower pressure peaks with respect to conventional diesel fuelling. Since the whole combustion process is shifted towards the expansion stroke, DF operation is characterized by pressure traces of higher values, in this phase, with respect to diesel mode.

Table 7
CoV of the measured quantities.

Measured quantity	CoV [%]
Air mass flow rate	1.3
Diesel mass flow rate	2.5
Methane mass flow rate	1.6
imep	4.0
Exhaust temperature	2.7
Engine speed	0.2
Engine torque	0.7
Particulate matter	3.0

A better understanding of combustion evolution is provided by ROHR evolution. In the operating conditions at 1600 rpm (Fig. 2-a), diesel operation shows two peaks due to the pilot and main combustion. Both peaks are visible also in DF mode even if their behavior is quite different because of the methane presence. DF mode has retarded start of combustion (SOC) of the pilot with respect to diesel operation; in particular, the combustion delay increase from 1.4 up to 2.4 cad when the load increase from 30% up to 70%. This trend could be ascribed to the increased methane concentration. The gas fuel, in fact, lowers the temperature in the chamber thus inhibiting the diesel ignition. Moreover, the longer diesel ignition delay is correlated to chemical factors due to the gas fuel presence. The methane mixed with air, in fact, alters the properties of the charge, the oxygen concentration and the pre-ignition reaction activities during compression [31]. After the pilot peak, DF main combustion starts before the end of pilot event as evidenced by the fact that it starts at higher ROHR values than conventional diesel mode (Fig. 2-a). This behavior is due to the flame propagation of the methane charge, ignited by the pilot diesel fuel, and then further promoted by main diesel fuel. Concerning the main combustion of diesel operation, it shows a first premixed peak followed by a diffusive phase. DF combustion, instead, occurs mainly in premixed way. In particular, in the first premixed phase, the ROHR traces of both modes are overlapped; then, DF combustion reaches slightly lower peak and exhibits a prolonged tail thus affecting the emissions oxidation. As result, more fuel is burnt in the last phase of combustion leading to higher temperature during expansion and exhaust stroke.

Similar considerations regarding the differences in combustion evolution between diesel and DF operation can be done also at 2800 rpm as shown in Fig. 2-b. DF combustion, in fact, has retarded pilot combustion. Main combustion starts before the end of pilot event and it is characterized by lower rate with respect to diesel operation because of the slower burning velocity of the gaseous fuel. Moreover, DF main combustion is more strengthened with respect to diesel operation. How DF combustion diverges from the diesel one is particularly evident at 2800 rpm–35 Nm where both premixed and diffusive phase are clearly distinguishable for diesel operation while DF combustion seems to occur essentially in premixed mode.

At 3200 rpm at all investigated loads (Fig. 2-c), there is no evidence of the pilot combustion for both diesel and DF operations maybe because of the lower amount of fuel injected during the pilot event at high engine speeds. The absence of the pilot combustion makes clearer the effect of methane on main combustion. In these operating conditions, in fact, the slower combustion rate of the gaseous fuel results in delayed and longer combustion with respect to diesel fuel.

Looking at bulk temperatures traces, for all operating conditions, it is observed that lower temperatures are detected during compression and the early expansion stroke for DF combustion. Then, higher temperatures are observed for DF operation because the combustion is moved towards the expansion stroke as ROHR curves have also confirmed.

In order to identify the effect of methane fuel on particle emissions, both particle number (PNSDF) and mass (PMSDF) size distribution functions were detected for diesel and diesel/methane operation at all the investigated conditions. The need to characterize particle number and size beyond particulate mass is due to the adverse effects of ultrafine particles (smaller than 100 nm) on environment and human health [32]. Figs. 3–5 show the PNSDFs and

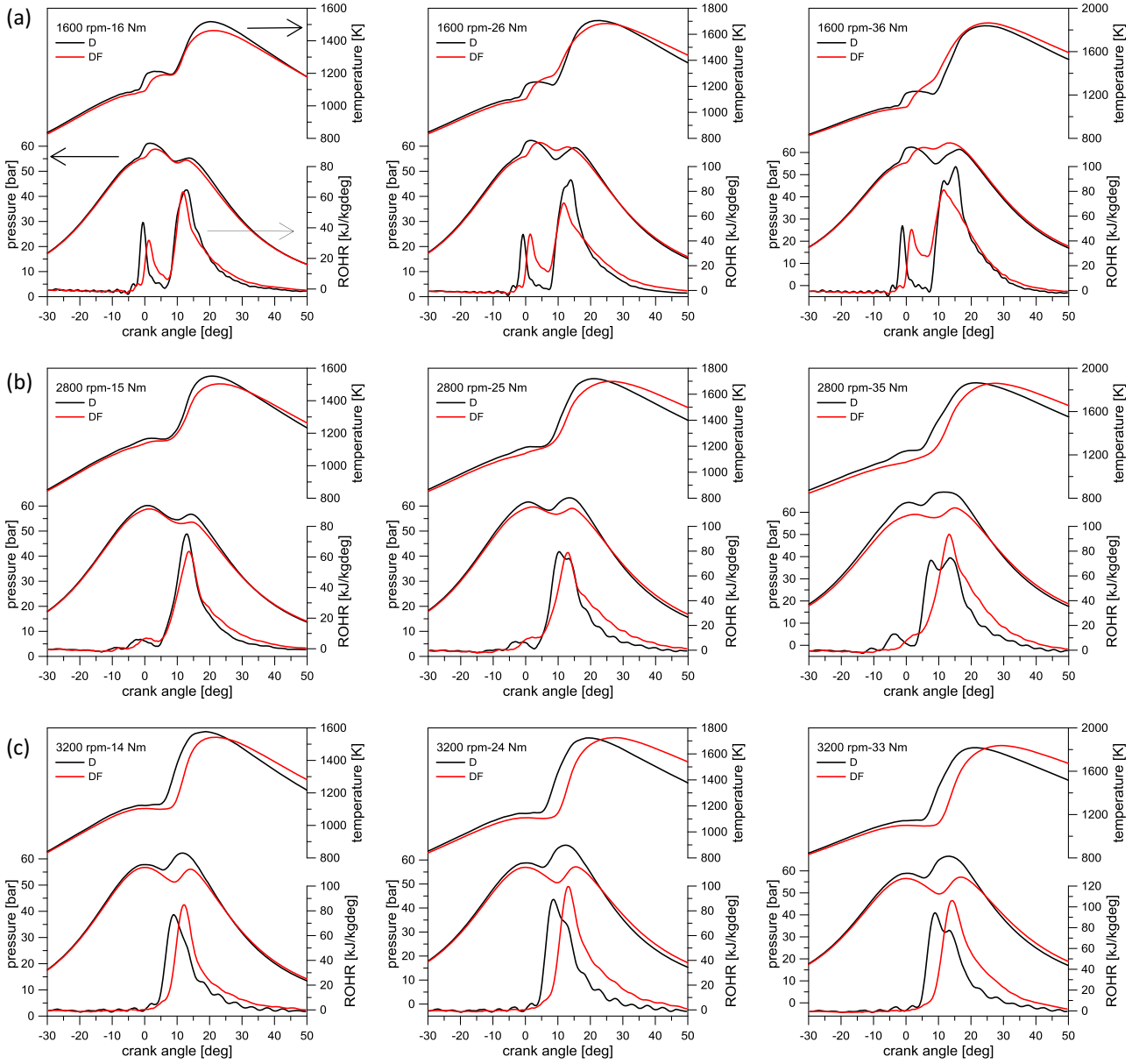

Fig. 2. In-cylinder pressure, ROHR and temperature for diesel and DF combustion at (a) 1600 rpm, (b) 2800 rpm, (c) 3200 rpm and at 30%, 50% and 70% of maximum load.

PMSDFs at 1600, 2800 and 3200 rpm, respectively, and at 30%, 50% and 70% of full load for each engine speed. It can be observed that particles range from 8 up to about 300 nm. PNSDFs exhibit unimodal or bimodal distributions depending on the operating condition: particles smaller than 20 nm are known as nucleation mode while particles larger than 20 nm are typical of accumulation mode. Nuclei particles are mainly due to semivolatile components originated from unburned fuel, lubricant oil and partial combustion products. Upon dilution and cooling in ambient air or during sampling, these vapors can either condense on pre-existing soot particles or nucleate to form nucleation mode particles. Accumulation particles consist of fractal-like carbonaceous agglomerates; these particles are formed in locally fuel-rich regions of the flame [33].

The mean particle diameter (D_m) and the total particle number (N) can be calculated from the PNSDFs. In particular, D_m is the weighted average of diameters at each particle size class:

$$D_m = \frac{\sum_{i=1}^{n} D_{p,i} \cdot N_i}{\sum_{i=1}^{n} N_i} \tag{4}$$

where n is the total number of particle size classes, D_p is the particle diameter and N_i is the particle number concentration at the ith particle size class. As the particle size classes are logarithmically spaced, to convert $dN/d\log D_p$ to N, it is necessary to divide by 16 as the concentration was normalized to 16 channels per decade:

$$N_i = \frac{dN_i/d\log D_p}{16} \tag{5}$$

By integrating the area under the curves $dN/d\log D_p$ over D_p, the total particle number can be obtained.

Moreover, the total mass, M, of the particles per unit volume of air sampled can be calculated as follows:

$$dM = dN \cdot (\pi/6) \cdot D_p^3 \cdot \rho \tag{6}$$

The mass concentration calculation assumes that all the particles are perfect spheres. The most of the particle mass falls in the accumulation mode: as typical for the PMSDFs, the curves peaks are shifted towards larger diameters with respect to the PNSDFs

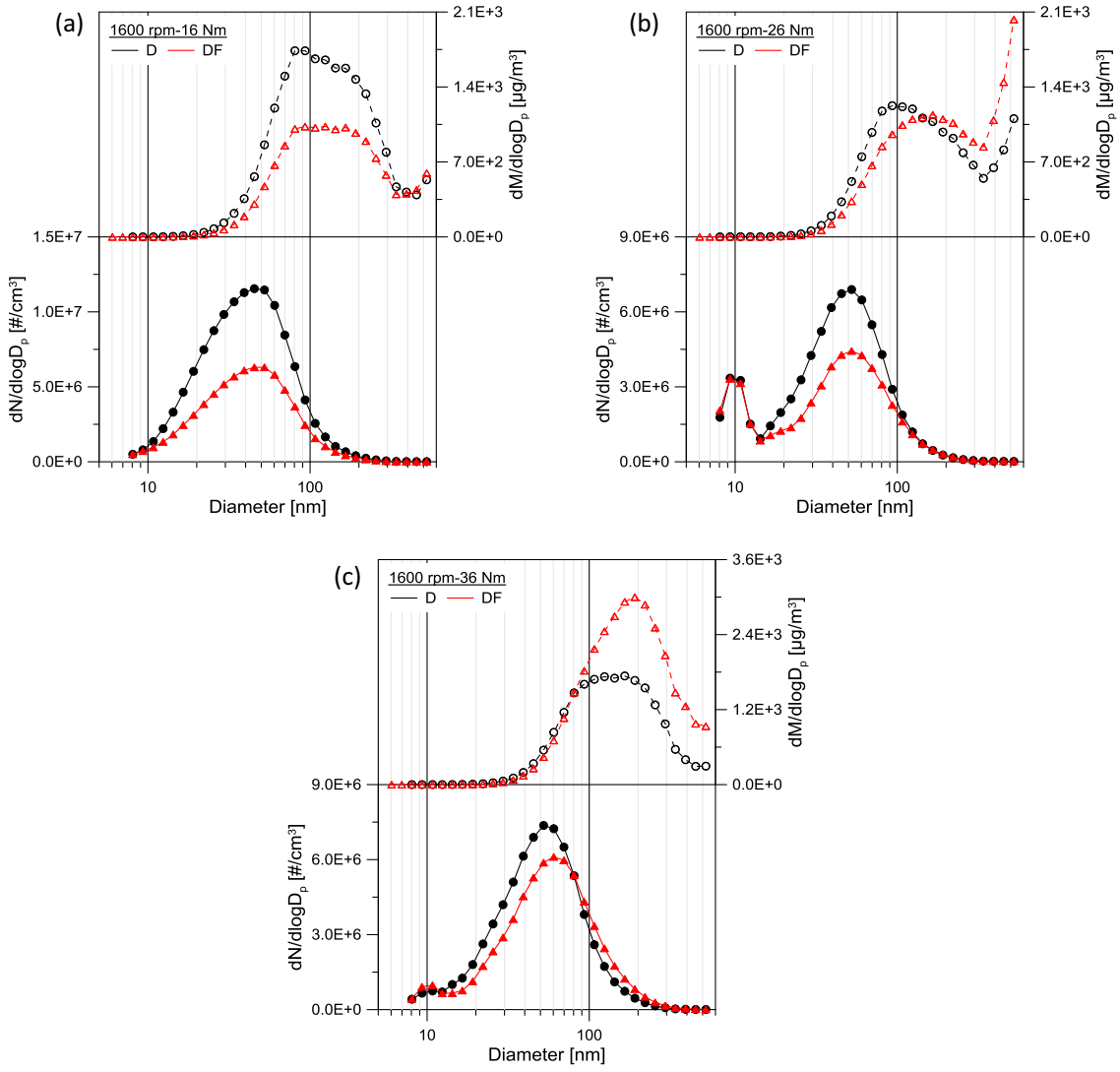

Fig. 3. PNSDF and PMSDF for diesel and DF operation at 1600 rpm and at (a) 30%, (b) 50% and (c) 70% of full load.

because large particles contribute much more to the total mass. The mass concentrations calculated by PMSDFs together with the ones measured by the smoke meter are reported in Fig. 6. It is worth underlining that the PM concentrations calculated from the data of EEPS and the smoke meter have different values due to the different measurement principle of the two instruments Nevertheless, PM concentrations measured with the two instruments show a good correlation as evidenced also by other authors [34]. Therefore, both PM concentrations can be considered for the purpose of comparison between diesel and DF operation since they show similar trend.

By looking at Fig. 3, it can be observed that PNSDFs of both diesel and DF mode exhibit a unimodal evolution at 30% of load while they are characterized by bimodal behavior at 50% and 70% of load. In the test point 1600 rpm–16 Nm, no significant differences are observed in the particle diameter between DF and diesel combustion. D_m is, in fact, 48 and 47 nm for DF and diesel fuel, respectively. The total particle number, instead, decreases from 1.3E8 for diesel down to 6.9E7 for DF. Lower particle number is emitted in DF mode since a part of diesel fuel is replaced by methane that should not have a primary role in the soot formation. The lower C/H ratio and the absence of C–C bonds of methane, in fact, reduce the soot formation tendency of the gaseous fuel. Therefore, DF combustion emits lower amount of particles whose size is similar to those produced by only diesel fuel thus resulting in lower mass concentration for DF operation. The lower tendency to soot formation in DF operation was also proved by optical investigation of combustion process. Combustion phase images acquired on an optically accessible CI engine, in fact, revealed low flame emission intensity when the engine runs in DF mode with respect to conventional diesel operation [35]. The flame emission intensity can be correlated to the soot concentration: the lowest is the flame luminosity the lowest is the soot concentration [36].

Concerning the PNSDFs detected at 1600 rpm–26 Nm, DF and diesel operation show similar nuclei mode while DF combustion emits lower amount of accumulation mode particles, 4.0E7 for DF versus 6.1E7 for diesel fuel, with larger diameter, 62 nm for DF versus 57 nm for diesel. The larger diameter could be ascribed to a different mechanism of particle formation for DF combustion with respect to diesel one. The cooling effect of methane, in fact, could worsen the pilot liquid fuel vaporization and its combustion efficiency. Moreover, in DF combustion the dwell time between the pilot and main combustion is too short to guarantee a good evaporation of the main diesel fuel thus resulting in larger particle

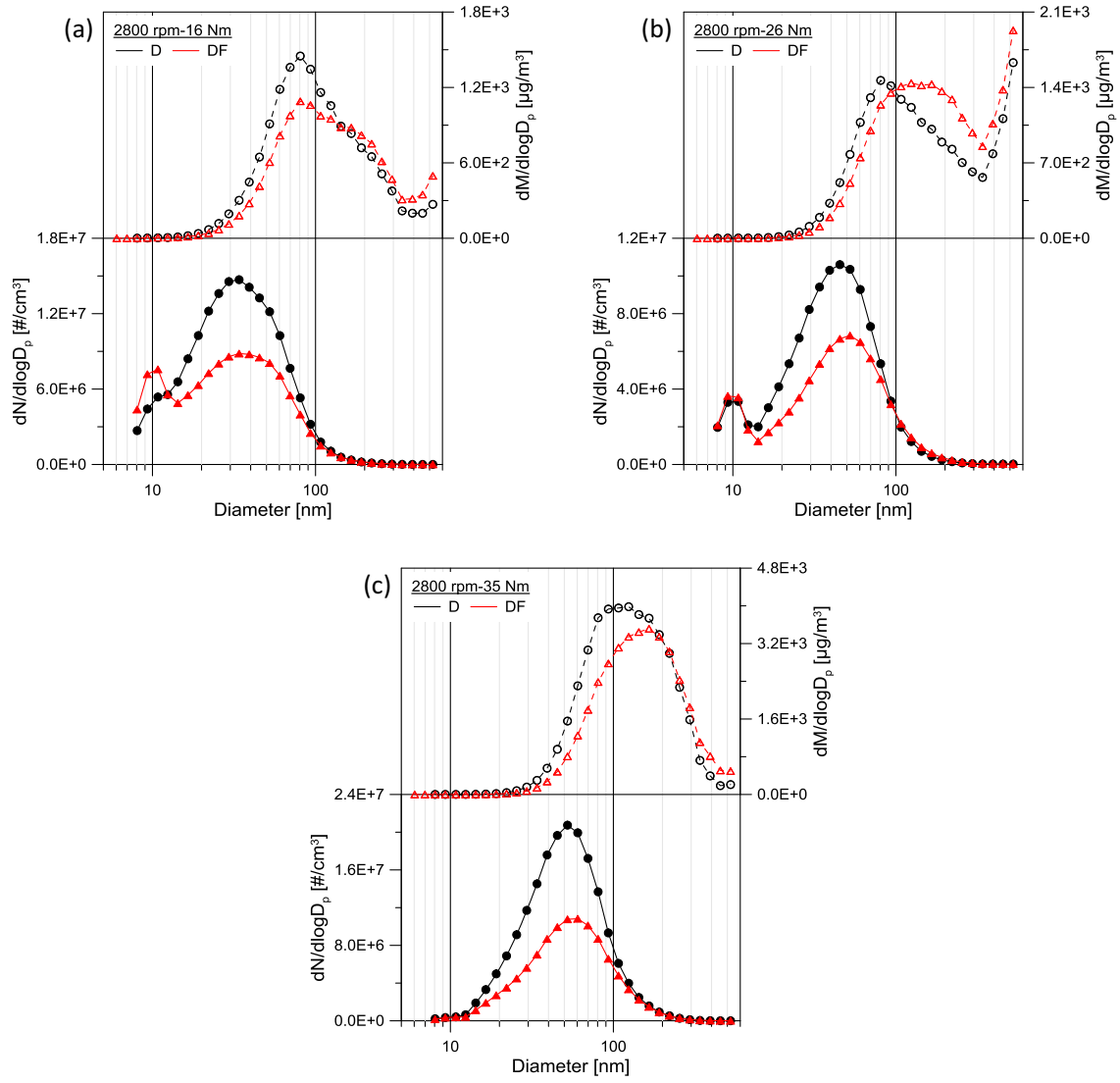

Fig. 4. PNSDF and PMSDF for diesel and DF operation at 2800 rpm and at (a) 30%, (b) 50% and (c) 70% of full load.

diameters (Fig. 2). Therefore, even if DF combustion emits lower number of particles their size is larger than diesel fuel thus leading to quite similar mass concentration for both operations.

Moving to higher load, (1600 rpm–36 Nm) it can be noted that nuclei modes behave in the same way for diesel and DF operation. Regarding to the accumulation mode, particle number of DF operation is slightly lower, 6.0E7, with respect to the diesel operation, 6.8E7; D_m is higher for DF, 71 nm versus 60 for diesel fuel. As consequence, the particulate mass concentration is increased for DF operation as also pointed out by the PMSDFs.

Similar considerations can be done at 2800 rpm: the PNSDFs shown in Fig. 4 exhibit bimodal behavior at 30% and 50% of full load while they are characterized just by accumulation mode at 70% of load. In particular, in the conditions at 30% and 70% of load, accumulation D_m is larger for DF than diesel fuel; however, the number of accumulation particles emitted by DF combustion is sufficiently lower so that the mass concentration is lower with respect to diesel operation. A different trend is observed at 50% of load where DF emits lower number of particles whose size is larger with respect to diesel fuel thus resulting in higher mass concentration.

An interesting behavior is observed at high engine speed (Fig. 5) where DF combustion is characterized by very pronounced nuclei mode and less evident accumulation mode with respect to diesel fuel. In particular, in the condition 3200 rpm–14 Nm, DF combustion emits 4.1E7 nuclei particles versus 1.4E7 for diesel fuel. Particle number in accumulation mode, instead, is reduced of about one order of magnitude for DF operation, 1.7E7 for DF versus 1.2E8 for diesel fuel. It is known from literature that carbonaceous agglomerates typical of the accumulation mode act as "sponges" that soak up volatile particles precursors [37]. In DF mode, since lower amounts of large particles are formed, the condensation and adsorption of the soluble organic fraction on soot particles are weakened and so more nuclei particles are produced.

The significant lower amount of accumulation particles emitted in DF mode at 3200 rpm with respect to the conditions at 1600 and 2800 rpm, could be correlated to different combustion behavior. Indicating data (Fig. 2-c) have, in fact, revealed that DF combustion occurs mainly in premixed mode and no peak due to pilot reacting fuel is detected. Moreover, the DF combustion is characterized by more lengthened combustion that enhance the particles oxidation. Since the main contribution to the total mass is given

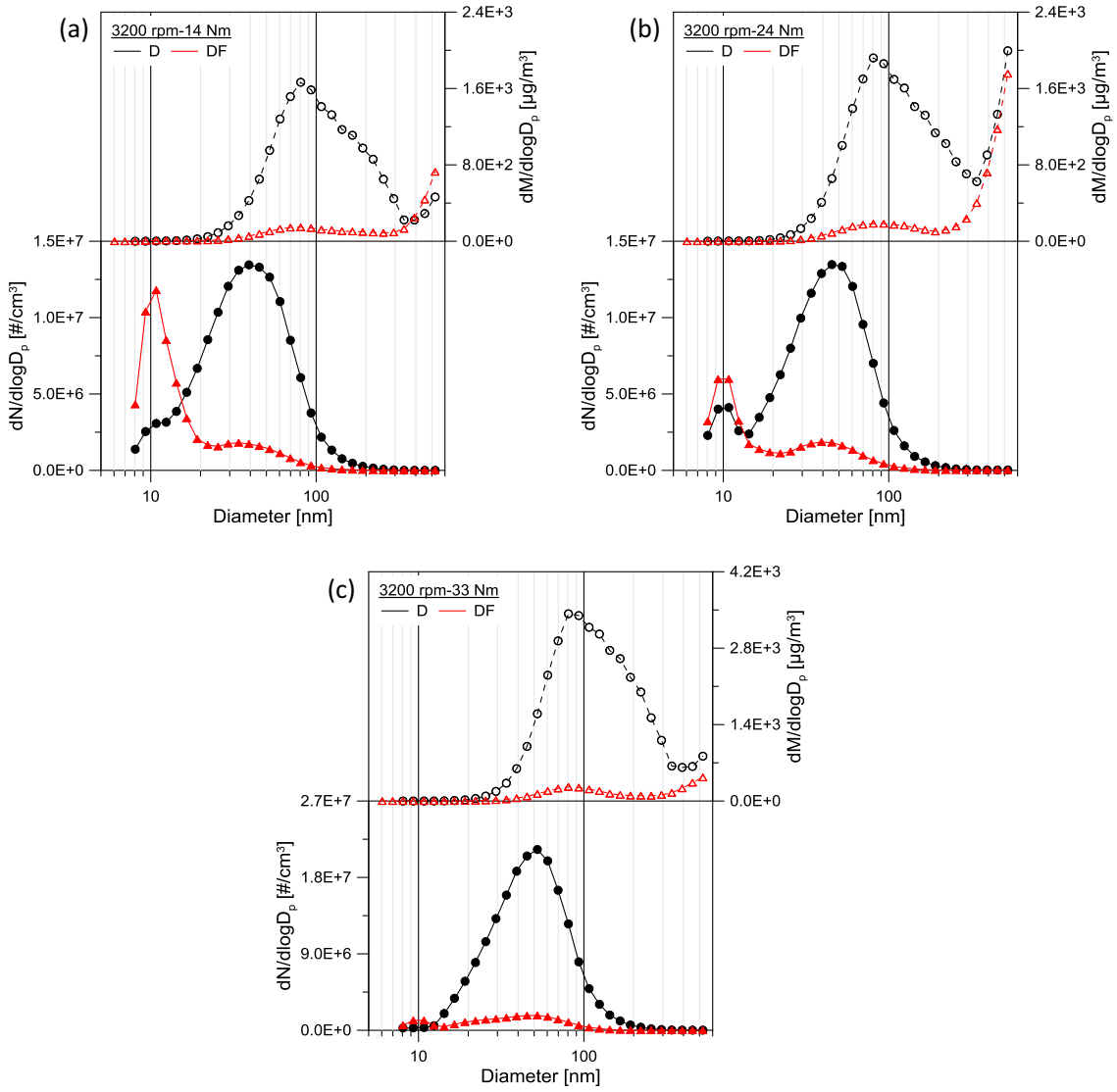

Fig. 5. PNSDF and PMSDF for diesel and DF operation at 3200 rpm and at (a) 30%, (b) 50% and (c) 70% of full load.

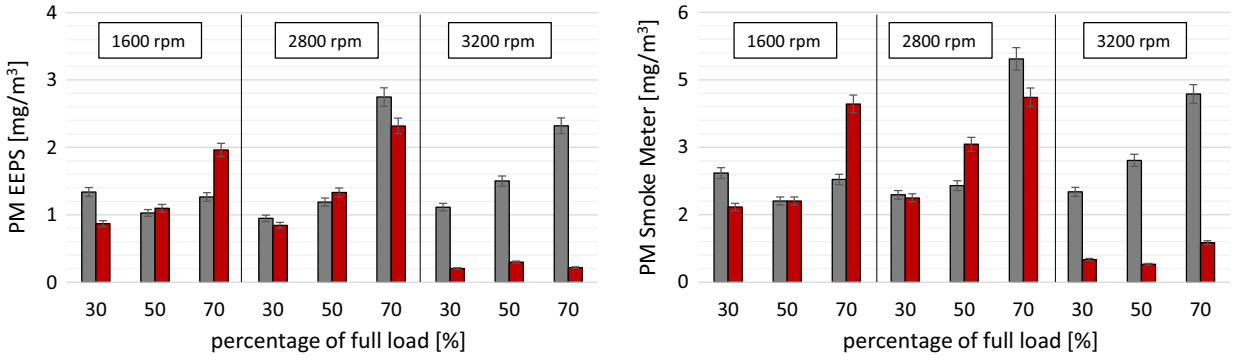

Fig. 6. PM concentrations measured by EEPS (left) and by smoke meter (right).

by accumulation particles, DF combustion is characterized by lower particle mass concentration than diesel fuel. This combustion behavior could reveal that the major responsible of particle emission at lower engine speeds is the diesel fuel and its worsened pilot combustion efficiency.

By looking to the data at 50% and 70% of load, it can be observed that the particle number typical of nuclei mode decreases when the load increases since the combustion temperature and the amount of injected fuel increases while the air/fuel ratio decreases. These conditions promote the precursor soot formation and at the

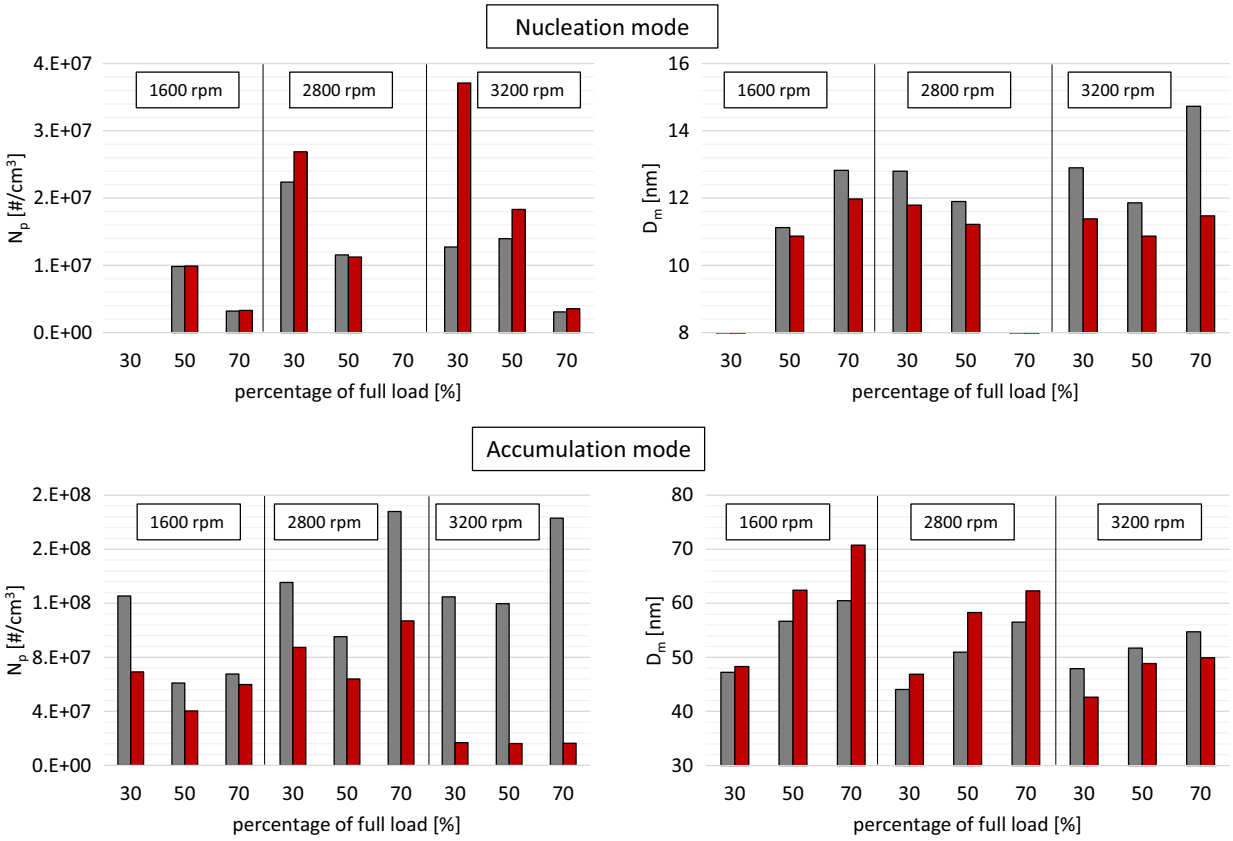

Fig. 7. Particle number and mean diameter for both nucleation (up) and accumulation mode (down).

same time accelerate the agglomeration process [38]. However, also at 50 and 70% of load, nuclei particles emitted by DF combustion are dominant while the number of accumulation particles is significantly reduced with respect to diesel operation thus resulting in lower mass concentration when the engine runs in DF mode.

In order to summarize the results concerning the particle emissions, the total particle number and the mean diameter categorized into nucleation and accumulation mode for both diesel and DF operation, at all exanimated conditions, are reported in Fig. 7. It is important to remark that the effect of diesel/methane combustion on particle formation is strongly related to the combustion evolution and, in particular, to the interaction between pilot and main combustion. At 1600 and 2800 rpm, it was observed a reduction of particle number and an increase of particle diameter in accumulation mode when the engine runs in DF mode. This behavior could be ascribed to a not very efficient diesel pilot combustion that affect also the main event, as evidenced by the shorter dwell time between the pilot and main combustion for DF mode (Fig. 2). At 3200 rpm, instead, there is no evidence of pilot combustion for both fuelling and, in particular, DF results in a more efficient main combustion. As consequence, at high engine speeds, DF operation emits a significantly lower number of particle whose size is smaller than those emitted by conventional diesel mode.

4. Conclusions

This study focuses on the performance, combustion evolution and exhaust emissions of a 1.0 L compression ignition engine modified to run in diesel/methane DF mode. Experiments were carried out at steady state conditions, at the engine speeds of 1600, 2800 and 3200 rpm and at 30%, 50% and 70% of full load. Indicating data were detected in order to investigate the differences in combustion evolution between DF and conventional diesel operation. PM emissions were measured at exhaust. Particular attention was payed to the effect of methane on both particle size, number and mass.

Indicating data have shown that DF operation is characterized by delayed combustion with respect to conventional diesel fuelling. In particular, methane induction at intake reduces the temperature and in-cylinder pressure of the fuel/air charge during the compression stroke resulting in lower pressure rise and peak values. The lower flame propagation of methane makes the combustion phase longer; thus, it is shifted towards the expansion stroke with respect to diesel fuel.

Regarding the effect of methane addiction to diesel fuel on ultrafine particle emissions, it was found out a clear dependence of particle number and mass size distributions from the combustion behavior and, in particular, from the interaction of pilot and main combustion phase.

At all investigated conditions, DF operation reduces the number of particles with respect to diesel operation while their size is correlated to the combustion evolution. In particular, at 1600 and 2800 rpm, the diameter of the particles emitted in DF mode is higher with respect to conventional diesel operation and they are mainly due to the effect of diesel pilot combustion. At high engine speed, instead, DF operation shows very pronounced nuclei mode and less evident accumulation mode. As result, DF combustion emits lower amounts of particles of smaller size.

From the present research activity, it was highlighted that DF combustion allows a reduction of total particle number with respect to diesel operation. This trend is particularly relevant with regards the issue of after-treatment filters since the use of methane fuel could slow down the clogging of the filters. Therefore, less frequent regeneration process could be necessary with benefit in terms of fuel consumption.

Acknowledgments

Authors are grateful to Mr. Carlo Rossi and Mr. Bruno Sgammato for the engine assessment and for the support in the experimental activity.

References

[1] Heywood JB. Internal combustion engine fundamentals. New York: McGraw-Hill; 1988.
[2] Datta A, Mandal BK. A comprehensive review of biodiesel as an alternative fuel for compression ignition engine. Renew Sustain Energy Rev 2016;57:799–821.
[3] Wei L, Geng P. A review on natural gas/diesel dual fuel combustion, emissions and performance. Fuel Process Technol 2016;142:264–78.
[4] Korakianitis T, Namasivayam AM, Crookes RJ. Natural-gas fueled spark-ignition (SI) and compression-ignition (CI) engine performance and emissions. Prog Energy Combust Sci 2011;37:89–112.
[5] Sahoo BB, Sahoo N, Saha UK. Effect of engine parameters and type of gaseous fuel on the performance of dual-fuel gas diesel engines – a critical review. Renew Sustain Energy Rev 2009;13:1151–84.
[6] Papagiannakis RG, Hountalas DT. Combustion and exhaust emission characteristics of a dual fuel compression ignition engine operated with pilot Diesel fuel and natural gas. Energy Convers Manage 2004;45:2971–87.
[7] Imran S, Emberson DR, Diez A, Wen DS, Crookes RJ, Korakianitis T. Natural gas fueled compression ignition engine performance and emissions maps with diesel and RME pilot fuel. Appl Energy 2014;124:354–65.
[8] Liu J, Yang F, Wang H, Ouyang M, Hao S. Effects of pilot fuel quantity on the emissions characteristics of a CNG/diesel dual fuel engine with optimized pilot injection timing. Appl Energy 2013;110:201–6.
[9] Di Iorio S, Magno A, Mancaruso E, Vaglieco BM. Performance, gaseous and particle emissions of a small compression ignition engine operating in diesel/methane dual fuel mode. SAE paper 2016-01-0771.
[10] Papagiannakis RG. Study of air inlet preheating and EGR impacts for improving the operation of compression ignition engine running under dual fuel mode. Energy Convers Manage 2013;68:40–53.
[11] Abedelaal MM, Hegab AH. Combustion and emission characteristics of a natural gas-fueled engine with EGR. Energy Convers Manage 2012;64:301–12.
[12] Yang B, Xi C, Wei X, Zeng K, Lai MC. Parametric investigation of natural gas port injection and diesel pilot injection on the combustion and emissions of a turbocharged common rail dual-fuel engine at low load. Appl Energy 2015;143:130–7.
[13] Paul A, Panua RS, Debroy D, Bose PK. Effect of compressed natural gas dual fuel operation with diesel and Pongamia pinnata methyl ester (PPME) as pilot fuels on performance and emission characteristics of a CI (compression ignition) engine. Energy 2014;68:495–509.
[14] Ryu K. Effects of pilot injection pressure on the combustion and emissions characteristics in a diesel engine using biodiesel-CNG dual fuel. Energy Convers Manage 2013;76:506–16.
[15] Mohsin R, Majid ZA, Shihnan AH, Nasri NS, Sharer Z. Effect of biodiesel blends on engine performance and exhaust emission for diesel dual fuel engine. Energy Convers Manage 2014;88:821–8.
[16] Li W, Liu Z, Wang Z. Experimental and theoretical analysis of the combustion process at low loads of a diesel natural gas dual-fuel engine. Energy 2016:728–41.
[17] Yang B, Wei X, Xi C, Liu Y, Zeng K, Lai MC. Experimental study of the effects of natural gas injection timing on the combustion performance and emissions of a turbocharged common rail dual-fuel engine. Energy Convers Manage 2014;87:297–304.
[18] Yousefi A, Birouk M, Lawler B, Gharehghani A. Performance and emissions of a dual-fuel pilot diesel ignition engine operating on various premixed fuels. Energy Convers Manage 2015;106:322–36.
[19] Bora BJ, Saha UK, Chatterjee S, Veer V. Effect of compression ratio on performance, combustion and emission characteristics of dual fuel diesel engine run on raw biogas. Energy Convers Manage 2014;87:1000–9.
[20] Carlucci AP, Laforgia D, Saracino R, Toto G. Combustion and emission control in diesel–methane dual fuel engines: the effects of methane supply method combined with variable in-cylinder charge bulk motion. Energy Convers Manage 2011;52:3004–17.
[21] Magno A, Mancaruso E, Vaglieco BM. Performance, combustion analysis of dual fuel operation in single cylinder research engine fuelled with methane and diesel. SAE paper 2015-24-2461; 2015.
[22] Carlucci A, Laforgia D, Saracino R, Toto G. Study of combustion development in methane-diesel dual fuel engines, based on the analysis of in-cylinder luminance. SAE paper 2010-01-1297; 2010.
[23] Maricq MM. Chemical characterization of particulate emissions from diesel engines: a review. J Aerosol Sci 2007;38:1079–118.
[24] Geng P, Yao C, Wei L, Liu J, Wang Q, Pan W, et al. Reduction of PM emissions from a heavy-duty diesel engine with diesel/methanol dual fuel. Fuel 2014;123:1–11.
[25] Pope CA, Dockery DW. Health effects of fine particulate air pollution: lines that connect. J Air Waste Manage Assoc 2006;56(6):709–42.
[26] www.dieselnet.com.
[27] Graves B, Patychuk B, Dastanpour R, Rogak S. Characterization on particulate matter morphology and volatility from a compression-ignition natural-gas direct-injection engine. Aerosol Sci Technol 2015;49:589–98.
[28] Millo F, Vezza D, Vlachos T, Fino D, Russo N, De Filippo A. Particle number and size distribution from a small displacement automotive diesel engine during DPF regeneration. SAE paper 2010-01-1552; 2010.
[29] TSI Engine Exhaust Particle Sizer (EEPS) Spectrometer Model 3090/3090AK. Instruction Manual.
[30] Holman JP. Experimental methods for engineers. New York: McGraw-Hill; 1994.
[31] Mustafi NN, Raine RR, Verhelst S. Combustion and emissions characteristics of a dual fuel engine operated on alternative gaseous fuels. Fuel 2013;109:669–78.
[32] Kittelson D, Kraft M. Particle formation and models in internal combustion engines. Cambridge Centre for Computational Chemical Engineering; 2014.
[33] Kittelson DB, Watts WF, Johnson JP. On-road and laboratory evaluation of combustion aerosols – Part 1: Summary of diesel engine results. J Aerosol Sci 2006;37:913–30.
[34] Khalek I, Premnath V. Comparison among DMS 500, EEPS SMPS, MSS, EC/OC, CPMA, using laboratory "Soot" particles. Cambridge Particle Meeting, July 3, 2015.
[35] Magno A, Mancaruso E, Vaglieco B. Combustion analysis of dual fuel operation in single cylinder research engine fuelled with methane and diesel. SAE technical paper 2015-24-2461; 2015.
[36] Magno A, Mancaruso E, Vaglieco BM. Endoscopic investigation of combustion process in a small compression ignition engine fuelled with rapeseed methyl ester. SAE paper 2014-01-2649; 2014.
[37] Kittelson D, Abdul-Khalek I. Formation of nanoparticles during exhaust dilution. In: EFI members conference fuels, lubricants engines, & emissions, January 18–20, 1999.
[38] Young LH, Liou YJ, Cheng MT, Lu JH, Yang HH, et al. Effects of biodiesel, engine load and diesel particulate filter on nonvolatile particle number size distributions in a heavy-duty diesel engine exhaust. J Hazard Mater 2012;199–200:282–9.